

Mutant KIT as imatinib-sensitive target in metastatic sinonasal carcinoma

S. M. Dieter^{1,2}, C. Heining^{1,2,3}, A. Agaimy⁴, D. Huebschmann^{5,6,7}, D. Bonekamp⁸, B. Hutter^{2,9}, K. R. Ehrenberg^{1,10}, M. Fröhlich^{2,9}, M. Schlesner⁵, C. Scholl^{1,2}, H.-P. Schlemmer⁸, S. Wolf¹¹, A. Mavratzas¹⁰, C. S. Jung¹², S. Gröschel^{1,2,3}, C. von Kalle^{1,2,3,13}, R. Eils^{5,6,13}, B. Brors^{2,9}, R. Penzel¹⁴, M. Kriegsmann¹⁴, D. E. Reuss¹⁵, P. Schirmacher^{2,14}, A. Stenzinger^{14,16}, P. A. Federspil¹⁷, W. Weichert^{14,18,19}, H. Glimm^{1,2,3} & S. Fröhling^{1,2,3*}

¹Department of Translational Oncology, National Center for Tumor Diseases (NCT) Heidelberg and German Cancer Research Center (DKFZ), Heidelberg; ²German Cancer Consortium (DKTK), Heidelberg; ³Section for Personalized Oncology, Heidelberg University Hospital, Heidelberg; ⁴Institute of Pathology, Erlangen University Hospital, Erlangen; ⁵Division of Theoretical Bioinformatics, DKFZ, Heidelberg; ⁶Department of Bioinformatics and Functional Genomics, Institute of Pharmacy and Molecular Biotechnology, and BioQuant, Heidelberg University, Heidelberg; ⁷Department of Pediatric Immunology, Hematology and Oncology, Heidelberg University Hospital, Heidelberg; ⁸Division of Radiology, DKFZ, Heidelberg; ⁹Division of Applied Bioinformatics, DKFZ and NCT Heidelberg, Heidelberg; ¹⁰Department of Medical Oncology, NCT Heidelberg, and Department of Internal Medicine VI, Heidelberg University Hospital, Heidelberg; ¹¹Genomics and Proteomics Core Facility, DKFZ, Heidelberg; ¹²Department of Neurosurgery, Heidelberg University Hospital, Heidelberg; ¹³DKFZ-Heidelberg Center for Personalized Oncology (HIPO), Heidelberg; ¹⁴Institute of Pathology; ¹⁵Department of Neuropathology, Institute of Pathology, Heidelberg University Hospital, Heidelberg, Germany; ¹⁶Department of Pathology, Center for Integrated Diagnostics, Massachusetts General Hospital, Harvard Medical School, Boston, USA; ¹⁷Department of Otorhinolaryngology, Heidelberg University Hospital, Heidelberg; ¹⁸Institute of Pathology, Klinikum rechts der Isar, Technische Universität München, Munich; ¹⁹DKTK, Munich, Germany

*Correspondence to: Prof. Stefan Fröhling, Department of Translational Oncology, NCT Heidelberg, Im Neuenheimer Feld 460, 69120 Heidelberg, Germany. Tel: 49.6221.56.35212; Fax: 49.6221.56.5389; E-mail: stefan.froehling@nct-heidelberg.de

Background: Sinonasal carcinomas (SNCs) comprise various rare tumor types that are characterized by marked histologic diversity and largely unknown molecular profiles, yet share an overall poor prognosis owing to an aggressive clinical course and frequent late-stage diagnosis. The lack of effective systemic therapies for locally advanced or metastatic SNC poses a major challenge to therapeutic decision making for individual patients. We here aimed to identify actionable genetic alterations in a patient with metastatic SNC whose tumor, despite all diagnostic efforts, could not be assigned to any known SNC category and was refractory to multimodal therapy.

Patients and methods: We used whole-exome and transcriptome sequencing to identify a KIT exon 11 mutation (c.1733_1735del, p.D579del) as potentially druggable target in this patient and carried out cancer hotspot panel sequencing to detect secondary resistance-conferring mutations in KIT. Furthermore, as a step towards clinical exploitation of the recently described signatures of mutational processes in cancer genomes, we established and applied a novel bioinformatics algorithm that enables supervised analysis of the mutational catalogs of individual tumors.

Results: Molecularly guided treatment with imatinib in analogy to the management of gastrointestinal stromal tumor (GIST) resulted in a dramatic and durable response with remission of nearly all tumor manifestations, indicating a dominant driver function of mutant KIT in this tumor. KIT dependency was further validated by a secondary KIT exon 17 mutation (c.2459_2462delATTCinsG, p.D820_S821delinsG) that was detected upon tumor progression after 10 months of imatinib treatment and provided a rationale for salvage therapy with regorafenib, which has activity against KIT exon 11/17 mutant GIST.

Conclusions: These observations highlight the potential of unbiased genomic profiling for uncovering the vulnerabilities of individual malignancies, particularly in rare and unclassifiable tumors, and underscore that KIT exon 11 mutations represent tractable therapeutic targets across different histologies.

Key words: precision oncology, cancer genomics, head and neck cancer

Introduction

The sinonasal cavities give rise to a variety of rare malignant neoplasms, primarily sinonasal carcinomas (SNCs), that differ significantly in etiology and pathologic characteristics and frequently carry a dismal prognosis due to diagnosis at advanced stages when radical surgery is infeasible [1]. SNCs can be subdivided by both histology and molecular features into an extremely heterogeneous group of neoplasms comprising intestinal and non-intestinal adenocarcinoma, squamous cell carcinoma (SCC), neuroendocrine carcinoma, SMARCB1-deficient carcinoma, lymphoepithelial carcinoma, NUT midline carcinoma (NMC), salivary gland-type carcinoma, sinonasal undifferentiated carcinoma (SNUC), and several other, even rarer tumor entities with only few reported cases worldwide [2–4]. The low incidence of SNC has hampered controlled prospective clinical trials, and as a consequence, optimal treatment for locally advanced and metastatic tumors remains unclear.

Several studies have provided insight into the genetic alterations associated with SNC, but the genomic ‘landscape’ of SNC is still poorly understood. In particular, aberrations that allow prediction of response to anticancer drugs or represent direct targets for therapeutic intervention are largely unknown, with the exception of targetable chromosomal rearrangements involving the *NUT* gene in NMC [5]. Additional potentially actionable molecular alterations identified in certain SNC subtypes include overexpression of the genes encoding EGFR, ERBB2, VEGF, and PTGS2 (also known as COX2) as well as amplification of the *FGFR1* locus [1, 6, 7]. However, the clinical utility of these putative therapeutic targets is still undetermined and awaits clinical validation. Thus, there is a strong unmet need for effective therapies in locally advanced and metastatic SNC.

Here, comprehensive molecular profiling in a patient with advanced-stage SNC refractory to multimodal treatment identified a *KIT* exon 11 mutation that provided a rationale for experimental treatment with imatinib, which led to a dramatic and long-lasting response.

Methods

Whole-exome and RNA sequencing

Tissue samples were provided by the NCT Heidelberg Tissue Bank. DNA and RNA were isolated using standard procedures. High-throughput sequencing and data analysis were performed as described [8, 9] (see also [supplementary methods](#), available at *Annals of Oncology* online for details). Exome and RNA sequencing data were deposited in the European Genome-phenome Archive under accession EGAS00001001845.

Histopathology

Formalin-fixed paraffin-embedded tissues were examined microscopically following staining with hematoxylin and eosin. Immunohistochemistry (IHC) was performed using standard protocols as detailed in [supplementary methods](#) and Table S1, available at *Annals of Oncology* online.

Study approval

Tumor tissue and a matched normal blood sample were obtained following written informed consent under an institutional review board-approved

protocol (S-206/2011) covering all aspects relevant to clinical cancer genome sequencing. This study was conducted in accordance with the Declaration of Helsinki.

Results

A 35-year-old man was diagnosed in 2013 with a locally advanced tumor that extended through the widened frontal recess into the right frontal sinus with crossing of the midline into the left ethmoid and frontal sinuses and descent into the right nasal cavity (Figure 1). The patient had neither been exposed to carcinogens associated with SNC nor to irradiation and did not have a family history of cancer.

Histologically, the tumor was composed of slightly polymorphic, medium-sized, rounded to elongated cells assembled in solid nests, which resulted in an overall entirely uncharacteristic appearance (Figure 2). There was no evidence of glandular, squamous, or any other type of differentiation. IHC showed diffuse strong immunoreactivity to antibodies against pancyokeratins, CK18, and epithelial membrane antigen. In addition, almost all tumor cells strongly expressed nuclear TP63 and both cytoplasmic and membranous CD117 (Figure 2). CD56 showed variable and patchy membranous reactivity in 15% of tumor cells (Figure 2); however, the specific neuroendocrine markers chromogranin A and synaptophysin were negative.

Due to the unusual profile of this neoplasm, an extended IHC panel was applied to test for any mesenchymal, neuroendocrine, or myoepithelial differentiation. The tumor cells were negative for vimentin, CK5/6, CK7, CD31, DOG1, CD34, CD99, S100, desmin, TTF1, GFAP, CD10, NUT, and hypophyseal hormone markers. Furthermore, SMARCB1 showed strong intact nuclear expression. There was no evidence of HPV and EBV gene expression or rearrangement of the *EWSR1* gene. TP53 showed nuclear expression in less than 10% of cells. The Ki-67 proliferative index was moderate (20%).

Based on these findings, we were unable to fit this neoplasm into any of the established SNC categories mentioned above. Specifically, large-cell neuroendocrine carcinoma was excluded as chromogranin A and synaptophysin were negative, CD56 expression showed a patchy nondiagnostic pattern, and the proliferative fraction was only moderately increased. Olfactory neuroblastoma was ruled out by the strong CK positivity and the lack of sustentacular cells on S100 staining. The absence of a broader set of myoepithelial markers and specific cytokeratins (CK5/6 and CK7) argued against solid-pattern adenoid cystic carcinoma and myoepithelial carcinoma. Although TP63 was positive, SCC was equally unlikely because of CK5/6 negativity and the lack of typical morphologic features. Furthermore, there was no morphologic or immunohistochemical evidence of NMC. Since CK7 was negative and proliferation was only modest, SNUC could not be diagnosed either. Angiosarcoma was ruled out by CD31 and CD34 negativity. Given that imaging studies revealed no evidence of other tumor manifestations, a metastasis was highly unlikely, and the case was ultimately diagnosed as solid carcinoma of the sinonasal cavity, not otherwise specified.

After radical surgery and adjuvant intensity-modulated radiotherapy (IMRT), there was no evidence of disease for 10 months until relapse occurred with dural tumor manifestations and

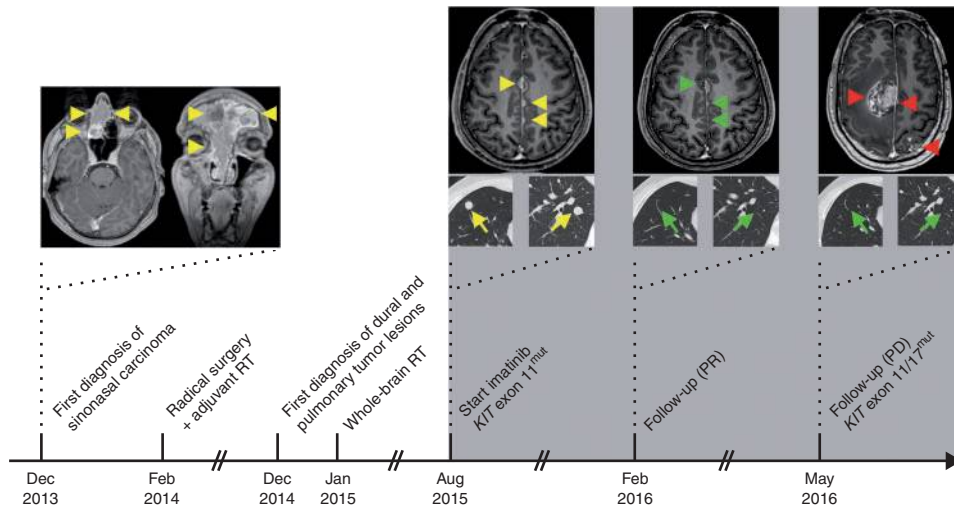


Figure 1. Course of disease. Left, axial and coronal contrast-enhanced, T1-weighted MR images of the brain depict the extent of the primary tumor. Middle and right, axial contrast-enhanced, T1-weighted MR images of the brain show response of nodular dural metastases to therapy (top); axial contrast-enhanced computed tomography (CT) images of the lung demonstrate response of pulmonary nodules to therapy (bottom). Arrows and arrowheads indicate actual or former tumor localizations. Yellow, lesions before imatinib treatment; green, responsive lesions; red, progressive lesions. RT, radiotherapy; PR, partial remission; PD, progressive disease.

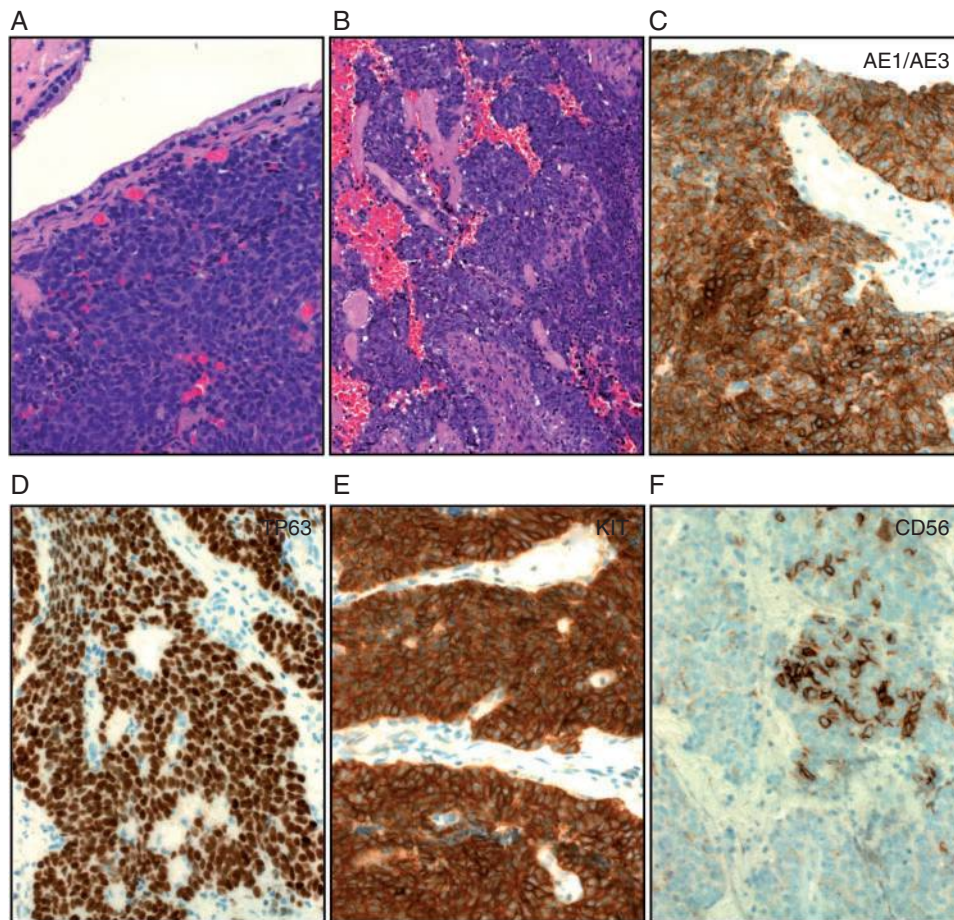


Figure 2. Histologic and immunohistochemical analysis of the patient tumor. Hematoxylin and eosin-stained tumor sections showed a small-round cell neoplasm with diffuse growth beneath the respiratory mucosa (A) and occasional superficial nesting/packageing and stromal hemorrhage (B). Immunohistochemistry showed diffuse strong expression of pancytokeratin (AE1/AE3) (C), nuclear TP63 (D), and CD117/KIT (E) in almost all tumor cells, but only very focal, patchy reactivity for CD56 (F). Original magnifications, $\times 200$.

Table 1. Somatic mutations identified by whole-exome sequencing

Chromosome	Position	Gene	RefSeq accession	Exon	Nucleotide change	VAF (DNA)	Protein change	VAF (RNA)	RPKM
SNV									
1p36.33	1 575 718	<i>CDK11B</i>	NM_033489	12	c.1063C>T	0.23	p.G355S	0.36	25.73
1p21.1	102 302 470	<i>OLFM3</i>	NM_058170	2	c.181C>A	0.46	p.A61S	0	0
1q43	241 798 585	<i>CHML</i>	NM_001821	1	c.484C>T	0.33	p.D162N	0.11	3.60
2p13.3	69 704 057	<i>AAK1</i>	NM_014911	21	c.2746C>A	0.31	p.D916Y	0	3.30
5q13.2	73 200 087	<i>ARHGEF28</i>	NM_001080479	32	c.4113 + 2T>A	0.39	Splice site	0	0.87
9q34.2	136 635 617	<i>VAV2</i>	NM_001134398	27	c.2230C>T	0.46	p.V744M	0.41	38.28
12q13.12	50 744 820	<i>FAM186A</i>	NM_001145475	4	c.5795G>A	0.35	p.P1932L	0	0.02
13q22.2	76 055 405	<i>TBC1D4</i>	NM_014832	2	c.498 + 1G>C	0.40	Splice site	0.57	7.10
20q13.12	46 267 869	<i>NCOA3</i>	NM_181659	14	c.2630C>T	0.07	p.P877L	0.07	8.27
22q13.31	46 931 726	<i>CELSR1</i>	NM_014246	1	c.1342C>T	0.36	p.E448K	0.51	23.23
Xq28	148 571 862	<i>IDS</i>	NM_000202	7	c.989G>A	0.70	p.A330V	0.90	20.37
Indel									
1p36.21	14 107 739	<i>PRDM2</i>	NM_012231	8	c.3450_3453del	0.25	p.K1151fs	0.43	58.81
1p36.21	14 108 370	<i>PRDM2</i>	NM_012231	8	c.4081_4083del	0.23	p.K1362del	0.36	58.81
1q24.3	172 558 628	<i>SUCO</i>	NM_016227	17	c.2841_2844del	0.21	p.N948fs	0.32	147.64
1q32.2	207 504 604	<i>CD55</i>	NM_001114752	6	c.817_819del	0.19	p.E273del	0.73	180.55
2q22.3	148 684 761	<i>ACVR2A</i>	NM_001616	11	c.1461_1463del	0.32	p.I489del	0.72	35.77
3p24.2	25 648 789	<i>TOP2B</i>	NM_001068	31	c.4153_4155del	0.16	p.N1385del	0.35	64.79
3q26.2	168 833 748	<i>MECOM</i>	NM_001164000	7	c.1344_1347del	0.23	p.K448fs	0.16	70.81
4p15.2	27 010 447	<i>STIM2</i>	NM_001169117	10	c.1313_1315del	0.17	p.K439del	0.38	143.61
4q12	55 593 666	<i>KIT</i>	NM_000222	11	c.1733_1735del	0.22	p.D579del	0.70	234.53
10p15.1	5 493 804	<i>NET1</i>	NM_001047160	4	c.268_269del	0.20	p.R91fs	0.44	247.23
19p13.11	18 967 038	<i>UPF1</i>	NM_002911	13	c.1754_1773del	0.18	p.L587fs	0.03	28.99

SNV, single-nucleotide variant; Indel, insertion/deletion mutation; VAF, variant allele frequency; RPKM, reads per kilobase of exon model per million mapped reads.

multiple small pulmonary metastases (Figure 1). Whole-brain IMRT with simultaneous integrated boost resulted in stabilization of the dural lesions for 6 months when there was evidence of progression with increasing and new dural and pulmonary metastases measuring up to 13 and 11 mm, respectively (Figure 1).

The value of chemotherapy in metastatic SNC has not been systematically analyzed, and extrapolation from retrospective studies indicating a potential benefit of induction chemotherapy in some SNC subtypes [1] was not appropriate as our patient's tumor could not be assigned to a known diagnostic category. Consequently, the choice of systemic treatment posed a challenge. To address the diagnostic uncertainty and possibly guide therapy, the patient was included in NCT Molecularly Aided Stratification for Tumor Eradication Research (MASTER), an institutional review board-approved clinical sequencing program for patients below the age of 51 years with advanced-stage cancer across all histologies and patients with rare tumors [8, 9]. Whole-exome sequencing of the primary tumor revealed 22 somatic mutations [11 single-nucleotide variants (SNVs) and 11 insertion/deletion mutations (indels)], and RNA sequencing demonstrated that 18 of the 22 mutated alleles were expressed (Table 1). Most striking from a clinical perspective was a heterozygous *KIT* exon 11 mutation (c.1733_1735del, p.D579del) that has previously been described in some cases of gastrointestinal stromal tumor (GIST) and melanoma as well as in one case of thymic carcinoma [10–12]. The presence of *KIT*

c.1733_1735del was confirmed by Sanger sequencing, and high *KIT* expression was verified by IHC (Figures 2 and 3).

Gain-of-function mutations that result in constitutive activation of the *KIT* receptor tyrosine kinase and its downstream effectors, such as the RAS-RAF-MAPK and PI3K-AKT signaling cascades, occur in a wide variety of cancers [13]. In particular, approximately 85% of GISTs are driven by *KIT* mutations (predominantly small indels), which affect exon 11 (juxtamembrane domain, 70%), exon 9 (extracellular dimerization motif, 20%), exon 13 (tyrosine kinase 1 domain, 1%–3%), or exon 17 (tyrosine kinase 2 domain and activation loop, 1%–3%) and confer sensitivity to small-molecule tyrosine kinase inhibitors (TKIs), as evidenced by a response rate of greater than 80% and a median event-free survival of nearly 24 months in patients with exon 11 mutant GIST that were treated with imatinib [14]. In contrast, entities such as melanoma or mastocytosis are usually associated with different types of *KIT* mutations (SNVs or gene amplifications) and variable sensitivities to pharmacologic *KIT* inhibition, illustrating that the potential of *KIT* to act as a dominant oncogenic driver is highly context-dependent [15, 16].

The p.D579del mutation identified in our patient, which is predicted to activate *KIT* through disruption of the autoinhibitory function of the juxtamembrane domain, was recently described in a patient with heavily pretreated thymic carcinoma who, upon progression on standard treatment, received imatinib

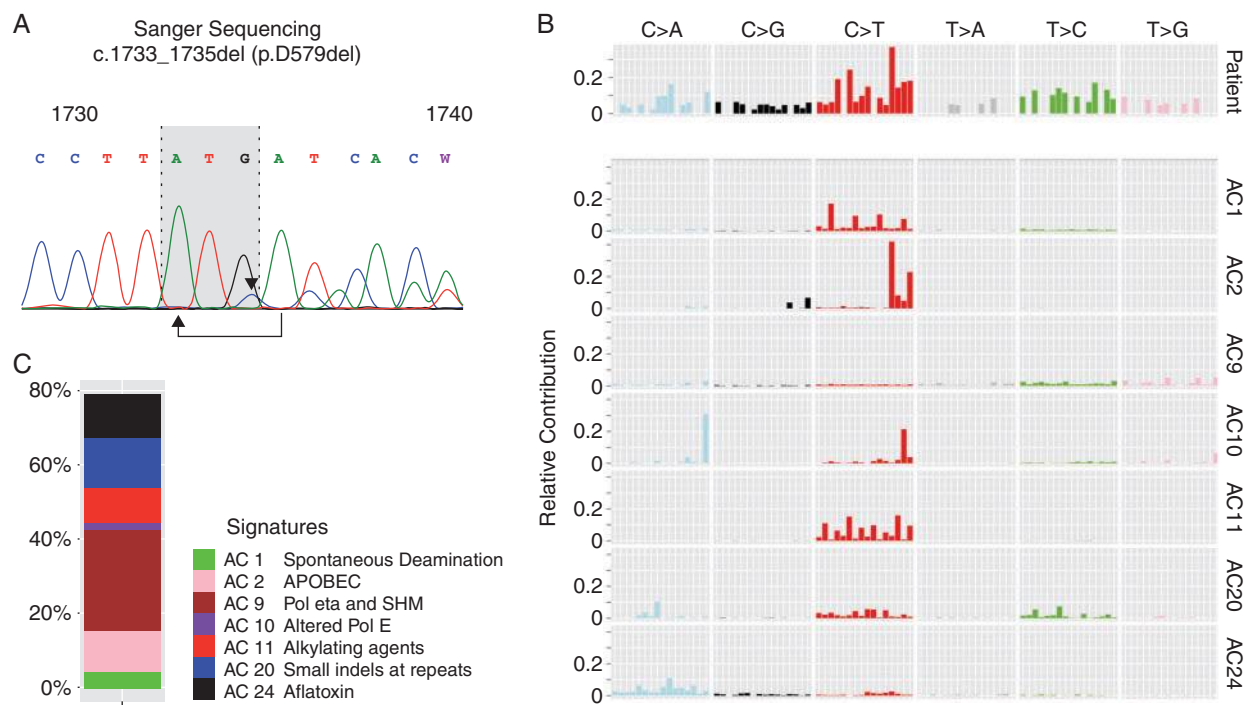


Figure 3. Validation of *KIT* exon 11 deletion and analysis of mutational signatures in the patient tumor. (A) Deletion of nucleotides 1733–1735 (gray box) in *KIT* exon 11 detected by Sanger sequencing. The DNA sequence change (arrow) and the first mismatched nucleotide (arrowhead) of the variant allele are indicated. Sequence numbering is according to NCBI Reference Sequence NM_000222. (B) Relative contribution of nucleotide exchanges in their triplet context to the mutational catalog of the patient tumor and to the different mutational signatures identified in the patient tumor. Mutational signatures are shown using a 96-substitution classification (horizontal axis) defined by the substitution class and the sequence context immediately 3' and 5' to the mutated base. The detailed classification is shown in [supplementary Figure 1](#), available at *Annals of Oncology* online. (C) Contribution of the signatures identified in the patient tumor to the overall mutational load. AC, Alexandrov-COSMIC signature; POL, polymerase; SHM, somatic hypermutation.

and experienced disease stabilization for at least 12 months [10]. This observation, together with the high overall sensitivity of *KIT* exon 11 mutations to TKI treatment in GIST, pointed to the therapeutic actionability of this mutation, and the patient was started on 400 mg imatinib daily. Therapy was well tolerated with no adverse effects other than grade 2 leukopenia that was stable during the course of treatment and did not require dose adjustment. After 2 months of therapy, computed tomography (CT) and magnetic resonance imaging (MRI) demonstrated complete resolution of all pulmonary lesions and partial regression with decreased contrast enhancement of the dural metastases, which diminished nearly completely after 6 months (Figure 1). Overall, a partial remission according to Response Evaluation Criteria in Solid Tumors was achieved, and the patient was in good condition without tumor- or treatment-related symptoms for 10 months.

Regrettably, follow-up MRI of the brain in May 2016 revealed new and increased dural tumor manifestations, while CT imaging of the lung demonstrated ongoing remission of all pulmonary metastases (Figure 1). Since approximately 70% of patients with *KIT* exon 11 mutant GIST and acquired imatinib resistance harbor secondary mutations in *KIT* [17], a progressive dural metastasis was subjected to sequencing of genomic hotspot regions frequently mutated in cancer. This analysis identified a complex indel (c.2459_2462delATTCinsG, p.D820_S821delinsG) in *KIT* exon 17, which encodes the activation loop of the *KIT* kinase domain. Given the low sensitivity to imatinib of *KIT* exon 17 mutations [17], this finding provided a molecular explanation for the

clinical observation of acquired resistance and validated mutant *KIT* as oncogenic driver and therapeutic target in this tumor. Preclinical and clinical evidence indicates that GIST patients with *KIT* exon 17 mutations are also resistant to standard second-line treatment with sunitinib [17]. In contrast, regorafenib was shown in a phase 3 study to induce partial response or disease stabilization in 75% of patients with imatinib- and sunitinib-refractory GIST [18]. While investigations into the genetic determinants of response were limited to primary *KIT* mutations in exon 9 and 11 in this study, the interim results of an ongoing phase 2 trial of regorafenib in GIST patients with secondary *KIT* exon 17 mutations showed an objective response rate of 80%, with partial remission in 5 of 15 patients and stable disease for more than 16 weeks in 7 of 15 patients [19]. Taken together, these data provide a rationale for salvage therapy with regorafenib in our patient.

In addition to informing choices regarding individualized therapies targeting distinct pathway vulnerabilities, genomic profiling can also provide insight into the etiology and molecular pathogenesis of cancers. Analysis of over 10 000 cancer exomes and 1000 cancer genomes has identified a continuously growing number of mutational signatures that shed light on the carcinogenic processes underlying different cancer types [20]. Supervised analysis can determine which of the known mutational signatures contribute to an individual tumor's mutational catalog, i.e. the spectrum of somatic point mutations in the context of the bases immediately 5' and 3' to each mutated base. In our patient, contributions of seven known signatures were detected (Figure 3, [supplementary Figure 1](#), available at *Annals of*

Oncology online), including two that are carcinogen-associated (signature Alexandrov-COSMIC [AC] 11, induced by alkylating agents; and AC24, induced by aflatoxins). This is in line with the fact that carcinogens are known to be involved in the etiology of most SNCs [1]. However, the specific carcinogens known to contribute to the development of SNC, i.e. wood or leather dust, have not yet been attributed to mutational signatures owing to the lack of published exome or whole-genome sequencing data from these tumors. Signature AC3, which results from defective repair of DNA double-strand breaks via homologous recombination and is predicted to be linked to platinum responsiveness [21], did not contribute to the tumor's mutational catalog, suggesting that platinum-based therapy would not have been beneficial to the patient.

Discussion

The KIT p.D579del mutation identified in our patient extends the spectrum of potential molecular targets in SNC and provides first evidence that genomics-guided therapy can be of value in this tumor entity. Furthermore, in view of recent observations that the suitability of oncogenic drivers as therapeutic targets may vary substantially depending on genetic and tissue context [15, 16], our observations underscore the importance of molecular case studies correlating individual genomic profiles with response to 'precision' treatment in various tumor entities. Specifically, the data indicate that variants affecting the regulatory function of the KIT juxtamembrane domain belong to the group of mutations that may be successfully targeted across different histologies, although their 'actionability' beyond GIST [14], thymic carcinoma [10], and SNC remains to be determined. In addition to providing a target for successful first-line systemic therapy, molecular analysis also identified a second-site *KIT* mutation in a metastatic lesion that escaped inhibition by imatinib. This finding explained the observed resistance, confirmed the strong KIT dependence of this tumor, and, most importantly, helped inform the choice of subsequent therapy, thereby highlighting the value of sequential molecular analyses in KIT-driven tumors irrespective of tissue origin.

As a first step to define the clinical utility of recent insights into the imprints left on cancer genomes by different carcinogenic processes [20], we have established a novel bioinformatics algorithm that enables supervised analysis of the contribution of known mutational signatures to an individual tumor's mutational catalog. We are confident that this approach can yield important diagnostic information and aid in therapeutic decision making, which can readily be tested in molecular stratification programs employing whole-exome or genome sequencing.

Finally, the excellent response to histology-agnostic treatment highlights the value of comprehensive genomic testing in patients whose tumors cannot be assigned to a specific diagnosis based on conventional criteria, which enables capturing a large spectrum of genetic alterations in an unbiased way to identify actionable mutations that are otherwise impossible to predict. To explore whether the present case of KIT-driven, poorly differentiated SNC may be indicative of a distinct tumor entity, analysis of additional cases with comparable clinical and histologic features will be needed.

Acknowledgements

The authors thank the DKFZ-HIPO and NCT Precision Oncology Program (POP) Sample Processing Laboratory, the DKFZ Genomics and Proteomics Core Facility, and the DKFZ-HIPO Data Management Group for technical support. We also thank Katja Beck, Karolin Willmund, Daniela Richter, and Peter Lichter for infrastructure and program development within DKFZ-HIPO and NCT POP. We thank Ivo Buchhalter and Nagarajan Paramasivam for establishing the workflow for somatic indel detection. Tissue samples were provided by the NCT Heidelberg Tissue Bank in accordance with its regulations and after approval by the Ethics Committee of Heidelberg University. DH is a member of the Hartmut Hoffmann-Berling International Graduate School of Molecular and Cellular Biology and of the MD/PhD Program of the University of Heidelberg.

Funding

This work was supported by grant H021 from DKFZ-HIPO and NCT POP [to C.H., H.G., S.F.].

Disclosure

The authors have declared no conflict of interest.

References

1. Llorente JL, Lopez F, Suarez C, Hermsen MA. Sinonasal carcinoma: clinical, pathological, genetic and therapeutic advances. *Nat Rev Clin Oncol* 2014; 11: 460–472.
2. Barnes L, Eveson JW, Reichart P, Sidransky D (eds). World Health Organization Classification of Tumours. Pathology and Genetics of Head and Neck Tumours. IARC Press: Lyon 2005.
3. Agaimy A, Koch M, Lell M et al. SMARCB1(INI1)-deficient sinonasal basaloid carcinoma: a novel member of the expanding family of SMARCB1-deficient neoplasms. *Am J Surg Pathol* 2014; 38: 1274–1281.
4. Bishop JA, Antonescu CR, Westra WH. SMARCB1 (INI-1)-deficient carcinomas of the sinonasal tract. *Am J Surg Pathol* 2014; 38: 1282–1289.
5. Bishop JA, Westra WH. NUT midline carcinomas of the sinonasal tract. *Am J Surg Pathol* 2012; 36: 1216–1221.
6. Gelbard A, Hale KS, Takahashi Y et al. Molecular profiling of sinonasal undifferentiated carcinoma. *Head Neck* 2014; 36: 15–21.
7. Udager AM, Rolland DC, McHugh JB et al. High-frequency targetable EGFR mutations in sinonasal squamous cell carcinomas arising from inverted sinonasal papilloma. *Cancer Res* 2015; 75: 2600–2606.
8. Kordes M, Roring M, Heining C et al. Cooperation of BRAF(F595L) and mutant HRAS in histiocytic sarcoma provides new insights into oncogenic BRAF signaling. *Leukemia* 2016; 30: 937–946.
9. Chudasama P, Renner M, Straub M et al. Targeting fibroblast growth factor receptor 1 for treatment of soft-tissue sarcoma. *Clin Cancer Res* 2016.
10. Hagemann IS, Govindan R, Javidan-Nejad C et al. Stabilization of disease after targeted therapy in a thymic carcinoma with KIT mutation detected by clinical next-generation sequencing. *J Thorac Oncol* 2014; 9: e12–16.
11. Origone P, Gargiulo S, Mastracci L et al. Molecular characterization of an Italian series of sporadic GISTs. *Gastric Cancer* 2013; 16: 596–601.
12. Satzger I, Schaefer T, Kuettler U et al. Analysis of c-KIT expression and KIT gene mutation in human mucosal melanomas. *Br J Cancer* 2008; 99: 2065–2069.
13. Ronnstrand L. Signal transduction via the stem cell factor receptor/c-Kit. *Cell Mol Life Sci* 2004; 61: 2535–2548.

14. Heinrich MC, Corless CL, Demetri GD et al. Kinase mutations and imatinib response in patients with metastatic gastrointestinal stromal tumor. *J Clin Oncol* 2003; 21: 4342–4349.
15. Carvajal RD, Antonescu CR, Wolchok JD et al. KIT as a therapeutic target in metastatic melanoma. *JAMA* 2011; 305: 2327–2334.
16. Lim KH, Tefferi A, Lasho TL et al. Systemic mastocytosis in 342 consecutive adults: survival studies and prognostic factors. *Blood* 2009; 113: 5727–5736.
17. Heinrich MC, Maki RG, Corless CL et al. Primary and secondary kinase genotypes correlate with the biological and clinical activity of sunitinib in imatinib-resistant gastrointestinal stromal tumor. *J Clin Oncol* 2008; 26: 5352–5359.
18. Demetri GD, Reichardt P, Kang YK et al. Efficacy and safety of regorafenib for advanced gastrointestinal stromal tumours after failure of imatinib and sunitinib (GRID): an international, multicentre, randomised, placebo-controlled, phase 3 trial. *Lancet* 2013; 381: 295–302.
19. Yeh C-N. Efficacy and safety of regorafenib in patients with metastatic and/or unresectable gastrointestinal stromal tumor harboring secondary mutation with exon 17: Interim report of a phase II trial. In ASCO annual meeting. *J Clin Oncol*; 2016: 34 (suppl; abstr e22511) 2016. <http://meetinglibrary.asco.org/content/169992-176>, (22 November 2016, date last accessed).
20. Alexandrov LB, Nik-Zainal S, Wedge DC et al. Signatures of mutational processes in human cancer. *Nature* 2013; 500: 415–421.
21. Alexandrov LB, Nik-Zainal S, Siu HC et al. A mutational signature in gastric cancer suggests therapeutic strategies. *Nat Commun* 2015; 6: 8683.